Biochemical Journal Immediate Publication. Published on 8 Sep 2006 as manuscript BJ20060668

NMR characterisation of the pH 4 beta intermediate of the Prion Protein:

The N-terminal half of the protein remains unstructured and retains a high degree of flexibility

Denis B.D. O' Sullivan[#], Christopher E. Jones[#,%], Salama R. Abdelraheim[$], Andrew R. Thompsett[$], Marcus W Brazier[$] Harold Toms[#], David R. Brown[$] and John H. Viles[*#]

[*]Corresponding Author:

[#]School of Biological and Chemical Sciences, Queen Mary, University of London Mile End Road, London E1 4NS, UK

j.viles@qmul.ac.uk Tel:(44) 020 7882 3054 Fax:(44) 020 8983 0973

[%]Current Address; Center for Metals in Biology, School of Molecular and Microbial Sciences, The University of Queensland, Brisbane, 4072, Australia.

[$]Department of Biology and Biochemistry, University of Bath, Bath BA2 7AY, UK

Key words: Folding intermediate; PrP; structure; CD; Diffusion; T_2 Relaxation

Running Title: pH 4 intermediate of the Prion Protein

Abbreviations: BSE, bovine spongiform encephalopathy; CJD, Creutzfeldt-Jacob disease; GPI, glycosyl-phosphatidylinositol; huPrP human PrP; mPrP mouse PrP; PrP, prion protein; PrP^C, cellular isoform of PrP; PrP^{Sc}, scrapie isoform of PrP.

Biochemical Journal Immediate Publication. Published on 8 Sep 2006 as manuscript BJ20060668

Abstract-

Prion diseases are associated with the misfolding of the prion protein (PrP) from a largely α-helical isoform to a β-sheet rich oligomer. Circular dichroism (CD) has shown that lowering the pH to 4 under mildly denaturing conditions causes recombinant PrP to convert from an α-helical protein to one that contains a high proportion of β-sheet like conformation. Here we characterise this soluble pH 4 folding intermediate using NMR. ^{15}N HSQC studies with mPrP(23-231) show that a total of ~150 dispersed amide signals are resolved in the native form, whereas only ~ 65 amide signals with little chemical shift dispersion are observable in the pH 4 form. 3D ^{15}N HSQC-TOCSY and NOESY spectra indicate that the observable residues are all assigned to amino acids in the N-terminus; residues (23-118). ^{15}N transverse relaxation measurements indicate these N-terminal residues are highly flexible with additional fast motions. These observations are confirmed via the use of truncated mPrP(113-231), which shows only ~sixteen ^{15}N HSQC amide peaks at pH 4. The loss of signals from the C-terminus can be attributed to line-broadening due to an increase in the molecular size of the oligomer or exchange broadening in a molten globule state.

Biochemical Journal Immediate Publication. Published on 8 Sep 2006 as manuscript BJ20060668

Introduction

Creutzfeldt-Jacob disease (CJD) in humans, bovine spongiform encephalopathy (BSE) in cattle and scrapie in sheep are fatal neurodegenerative diseases. The infectious agent of these diseases is devoid of nucleic acid and is almost entirely composed of the prion protein, PrP^{Sc}, which is a misfolded form of a cellular prion protein PrP^{C} [1]. The misfolding and folding intermediates of PrP are therefore of significant interest to those studying the mechanism of Prion replication. Recently it has been shown that it is possible to take synthetic recombinant PrP^{C} and cause it to misfold so that it can act as a seed for subsequent prion propagation after inoculation in transgenic mice overexpressing PrP^{C} [2].

The mature form of the benign mammalian prion protein is a ~208 residue glycoprotein that possesses two N-glycosylation sites and one disulfide bridge. After transportation through the secretory pathway, PrP^{C} is tethered to the cell surface via a GPI anchor at the C-terminus [1]. Three dimensional NMR solution structures of PrP^{C} from a number of mammalian species have been reported [3-6] which show that PrP^{C} consists of two structurally distinct domains. The N-terminal domain (residues 23 to 125) is highly disordered [7] and is notable for its ability to bind Cu^{2+} ions at pH 6 and above [8-12]. The N-terminus contains a highly conserved octa-repeating sequence, PHGGGWGQ between residues 57 and 90. The C-terminal domain (residues 126-231) is predominantly helical, containing 3 α-helices (residues 144-154, 175-193 and 200-219) as well as two short anti-parallel β-strands (residues 128-131 and 161-164).

The conversion of native PrP^{C} to its misfolded isoform PrP^{Sc} is accompanied by a number of biophysical changes. PrP^{C} is monomeric and readily susceptible to proteolysis with proteinase K but PrP^{Sc} forms insoluble aggregates that are resistant to proteinase K digestion [13-15]. Furthermore infra-red spectroscopy show that while PrP^{C} is predominately α-helical, PrP^{Sc} possesses a considerable amount of β-sheet structure [16, 17].

An early circular dichroism (CD) study on the unfolding behaviour of mouse PrP(121-231) indicated that the structural domain of PrP undergoes a transition from the native folded form (at neutral pHs) to a stable soluble conformational intermediate rich in β-sheet at pH 4 under mildly denaturing conditions (3.5 M urea) while at pH 2 only the unfolded form was present [18]. Similarly, an unfolding study performed on human PrP(90-231) using guanidine hydrochloride as denaturant showed the existence of a stable β-intermediate between pH 3.5 and 4.0 [19]. Subsequent studies confirmed the presence of the huPrP(90-231) β-intermediate and also

highlighted the necessity of having NaCl present for the formation of this β-intermediate in urea [20, 21].

Studies by Baskakov and others have shown that PrP (with its disulphide bond intact) can fold in one of three forms. Firstly the α-helix rich, soluble monomeric form, PrP^C, is rapidly formed under near neutral non-denaturing conditions [3-6]. Secondly a high molecular weight multimer that forms amyloid fibres is favoured under neutral pH, moderately denaturing conditions and agitation [22]. The third form is a soluble species favoured at low pH (~4) under moderately denaturing conditions with a high salt content [20, 21, 23]. This latter soluble species has a high β-sheet content as indicated by CD [18-21, 23]. Size exclusion chromatography suggests this soluble oligomer is octameric [22] while light scattering experiments suggest that this oligomer contains 8-15 monomers [24] or higher molecular mass species [21, 25].

Polymorphism at residue 129 is a key determinant of susceptibility to sporadic and acquired prion diseases. Recent studies have shown stability of the native α-helical PrP is unaffected by polymorphism at 129 (Met129 or Val129) [26]. However the presence of Valine at position 129 accelerates fibril formation at pH 7 [27], while conversely Met129 favours the formation of the pH 4 soluble intermediate [28]. Interestingly, only individuals homozygous for methionine at 129 (Met/Met) have contracted variant CJD [29]. Prion propagation in transgenic mice is triggered by preparations containing fibrils [2], although the toxic form is likely to be smaller protofibrils [30].

Structural details, on a per-residue basis, are lacking for the pH 4 folding intermediate, despite its importance in influencing the susceptibilities to prion propagation. We therefore aim to characterise the pH 4-intermediate using NMR methods. Chemical shift dispersion in 3D ^{15}N-HSQC-TOCSY experiments will indicate the extent of folding of PrP. ^{15}N transverse relaxation measurements will provide information on the flexibility of the pH 4 intermediate main-chain and ^{1}H translational diffusion will indicate its molecular size.

Biochemical Journal Immediate Publication. Published on 8 Sep 2006 as manuscript BJ20060668

Experimental Procedures

Expression and purification of recombinant mPrP(23-231) and mPrP(113-231) - Tag free and C-terminally His-tagged full-length mouse PrP(23–231) were cloned into a pET-23 vector as previously described [31]. In addition a truncated PrP fragment, PrP(113-231) was expressed which lacks the natively unstructured N-terminal domain. The proteins were expressed in 2-liter flasks of Escherichia coli BL21(DE3) cells in ^{15}N labeled minimal medium containing (1 g/l) $^{15}NH_4Cl$ (Cambridge isotope laboratories, Inc.). Cultures were grown at 37 ^{o}C to an A_{600} of 0.9 and the protein expression was induced by the addition of isopropyl-β-D-thiogalactopyranoside to a final concentration of 1 mM. Bacterial pellets were harvested after 4 hours and sonicated in Buffer A containing 8 M urea, 200 mM NaCl, and 50 mM Tris, pH 7.6. The resulting solution was cleared of bacterial debris by centrifugation at 15,000 rpm for 15 min. The protein (Tag-free or His-tagged) was absorbed to a copper-charged metal affinity column made from chelating Sepharose (Amersham Biosciences). The proteins were washed with at least 20 column volumes of Buffer A and eluted from the column using Buffer A supplemented with 300 mM imidazole. The protein was found to be greater than 95 % pure by polyacrylamide electrophoresis and Coomassie staining. The protein was refolded by successive rounds of dilution in deionised water and concentrated in a Vivaspin centrifugal concentrator (Vivascience) with a 10,000 molecular weight cut off. The refolded protein was dialysed twice at 4 ^{o}C against deionised water to remove residual urea. The concentration of mPrP(23-231) was measured by its absorbance at 280 nm with a theoretical extinction coefficient of 62,280 $M^{-1}cm^{-1}$ [32] and confirmed by BCA assay (Sigma).

Preparation of samples- NMR samples of full-length mPrP(23-231) were prepared in four different buffer systems. Samples of native His-tagged and tag-free mPrP(23-231) were prepared in 20 mM sodium acetate at pH 5.2. A β-intermediate sample of mPrP(23-231) was generated by preparing the protein in 3.5 M Urea, 150 mM NaCl, and 20 mM sodium acetate at pH ~3.9 (between pH 3.7 and 4.4). An acid denatured sample of mPrP(23-231) was made by preparing the protein in 3.5 M urea, 150 mM NaCl and 20 mM sodium acetate at pH 1.82. The fourth condition, using tag-free mPrP(23-231) and mPrP(113-231) at pH ~3.9 with a raised temperature of 37 ^{o}C in 20 mM sodium acetate instead of denaturant. The NMR samples contained 90% (v/v) H_2O/10% (v/v) D_2O and 0.005% (w/v) sodium azide to inhibit bacterial growth. Protein concentrations for NMR experiments were ~5 mg/ml.

NMR Spectroscopy- All NMR spectra were acquired at 30 ºC (or 37 ^{o}C when stated) on a Bruker Avance spectrometer operating at 600.1 MHz for ^{1}H nuclei using a 5 mm inverse detection

triple-resonance z-gradient probe. Phase sensitive 2D ^{15}N-HSQC spectra were acquired using Echo-antiecho gradient selection. ^{1}H acquisition parameters were 0.122 seconds acquisition time, 1 second fixed delay and 2048 complex (t_2) points while 256 complex points were collected for the^{15}N dimension. Thirty two transients were recorded for each t_1 interval. The ^{1}H and ^{15}N dimensions possessed spectral widths of 14 ppm and 25 ppm respectively. The ^{15}N dimension was zero filled to 256 data points before squared cosine apodisation and Fourier transformation.

Resonance assignments of the pH 4 intermediate were obtained using phase sensitive 3D ^{15}N-HSQC-NOESY [33] and ^{15}N-HSQC-TOCSY spectra [34] using Echo-antiecho gradient selection. The 3D ^{15}N-HSQC-TOCSY and 3D ^{15}N-HSQC-NOESY spectra were obtained using a mixing time of 60 ms and 150 ms respectively. For both experiments, 2048 complex points were collected in the direct ^{1}H dimension over a spectral width of 12 ppm. 64 complex points and 160 complex points were collected for the indirect ^{15}N and ^{1}H dimensions respectively over a ^{15}N spectral width of 25 ppm and a ^{1}H spectral width of 12 ppm in both experiments. Both spectra were zero filled to 2048 data points in the direct ^{1}H dimension, 128 data points in the indirect ^{15}N dimension and 512 data points in the indirect ^{1}H dimension. All NMR data was processed in XWINNMR (Bruker) and analysed in XEASY running on a Silicon Graphics O2 computer (SGI). Resonance assignments were made manually using sequential ^{1}H nOe connectivities.

^{15}N spin spin T_2 relaxation times were obtained from running phase-sensitive 2D ^{15}N-HSQC spectra acquired with Echo/antiecho gradient selection as described above. The variable relaxation delays used were 0.016, 0.032, 0.048, 0.064, 0.096, 0.128, 0.196 and 0.256 seconds [35]. ^{15}N transverse relaxation times were obtained by fitting 2D signal volumes or peak heights [36] to the following exponential decay curve: $I_t = I_0 e^{-t/T2}$, I_t is the 2D signal intensity at time t, I_0 is the initial 2D signal intensity and T_2 is the transverse relaxation time (Note, $T_2=1/R_2$).

Translational diffusion experiments were carried out using the stimulated echo (STE) method incorporating bipolar gradients to reduce eddy current effects [37, 38]. The gradient strength was calibrated using the value of 2.299×10^{-5} cm^2 s^{-1} as the translation diffusion constant for H_2O at 25 ºC. Water in the protein samples was suppressed with a 3-9-19 WATERGATE sequence. A spoiler gradient of 17.13 % was applied at the start of the diffusion time Δ. For protein and water diffusion measurements, the total duration of the gradient pulse δ was 0.006 s and 0.002 s respectively. For both measurements the time between gradients (Δ) was 0.1 s. An exponential line-broadening function (1 Hz) was applied prior to Fourier transformation. The integral of the baseline corrected

amide/aromatic region of the proton spectra were measured at sixteen different gradient strengths (G) ranging from 0.741 to 35.21 G/cm and fitted to the following equation:

$$\ln(I) = \gamma_H^2\delta^2G^2(\Delta-\delta/3)D_t + \ln(I_0)$$

I_0 is the initial integral, I is the measured integral, D_t is the translational diffusion coefficient (cm^2/second), and γ_H is the ^1H gyromagnetic ratio (2.675197×10^4 G^{-1} s^{-1}) [37, 38]. Plotting ln(I) against G^2 produces a straight line whose slope divided by $\gamma_H^2\delta^2(\Delta-\delta/3)$ yields D_t. The D_t values for H_2O in the native, β-intermediate and acid denatured samples of mPrP(23-231) were $2.30\pm0.01 \times 10^{-5}$ cm^2 s^{-1}, $1.87\pm0.01 \times 10^{-5}$ cm^2 s^{-1} and $1.89\pm0.01 \times 10^{-5}$ cm^2 s^{-1} respectively. The small decrease in the latter two D_t values for water was presumably due to the increased viscosity of these solutions arising from the presence of 3.5 M Urea. In order to correct for this effect, the D_t value of the β-intermediate form of mPrP(23-231) was multiplied by 1.23 (2.30/1.87) while the D_t value of the acid denatured form of mPrP(23-231) was multiplied by 1.22 (2.30/1.89). Similarly there was also a small correction made for D_t measurements recorded at 37 ^oC. The D_t values for H_2O in 20 mM sodium acetate at 30 °C and 37 °C were $2.35\pm0.01 \times 10^{-5}$ cm^2 s^{-1} and $2.71\pm0.01 \times 10^{-5}$ cm^2 s^{-1} respectively. The D_t value at 37 °C was therefore corrected by a factor of 1.15 (2.71/2.35) for a direct comparison of diffusion coefficient at the two temperatures.

Circular Dichroism Spectroscopy- Circular Dichroism (CD) spectra were recorded in the far-UV region (185-260 nm) at 25 °C in a 0.02 cm path-length cuvette (for samples containing urea) on an AVIV 202 CD spectrometer. CD spectra of tag-free mPrP(23-231) and (His-tagged) mPrP(113-231) (urea free) were recorded in the far-UV region at 37 ^oC in a 0.1 cm path-length cuvette on an Applied Photophysics Chirascan CD Spectrometer. Protein samples were prepared by diluting an aliquot from each of the NMR samples described previously with the appropriate buffer system. Spectra were recorded using three to four scans, a bandwidth of 1 nm and a wavelength step of 0.5 nm. CD spectra were background corrected and smoothed using AVIV software; smoothing for the urea free samples was not required. The protein concentration of CD samples was measured using the absorbance at 280 nm. Estimates of percentage secondary structure were obtained using the K2D and CDSSTR analysis programs available on the Dichroweb website [39]. CD spectra are presented as mean residue molar circular dichroism $\Delta\varepsilon_{MRE}$ units (M^{-1} cm^{-1}).

Results

2D ^{15}N-HSQC and Circular Dichroism Spectroscopy of mPrP(23-231)- Chemical shift dispersion in NMR is a powerful method of determining the extent of structure in proteins on a per-residue basis [40-42]. For this reason 2D ^{15}N-HSQC was used to characterize the folding of PrP under various conditions. The 2D ^{15}N-HSQC spectrum of native mPrP(23-231) (Figure 1A) possesses amide ^{1}H signals in the ^{1}H dimension from ~6.5-9.5 ppm, characteristic of a folded protein [40-42]. However, for conditions promoting formation of the β-intermediate i.e. 3.5 M Urea, 150 mM NaCl at pH 4.1 (Figure 1B), ^{1}H signals lie between 7.8 and 8.7 ppm. This contraction in the chemical shift dispersion is typical of a completely unfolded protein [40-42]. The 0.9 ppm ^{1}H dispersion range for amides in the 2D^{15}N-HSQC of mPrP(23-231) was very similar to that of the acid denatured species (Figure 1C), although the chemical shifts of the amide resonances are not the same. An aliquot from each of the three NMR samples was prepared for UV-CD spectroscopy. The CD spectrum of native mPrP(23-231), Figure 2A, is typical of a protein possessing α-helices. However, the CD spectrum taken from the NMR sample of mPrP(23-231) under β-intermediate forming conditions, is characteristic of a β-sheet species with a strong negative CD band at ~217 nm (Figure 2B). The acid denatured spectrum, Figure 2C, shows less ellipticity suggesting a more random conformation.

pH 4 Intermediate created at 37 ^{o}C - A recent study has indicated that the pH 4 intermediate can also be produced in the absence of chemical denaturant by simply raising the temperature to 37 ^{o}C [24, 25]. Figure 3A shows the 2D ^{15}N-HSQC of mPrP(23-231) at pH 3.6 incubated for ~2 hours at 37 ^{o}C. Incubation of the NMR sample for a further 30 hours caused no further change in the 2D ^{15}N-HSQC spectra. A CD spectrum of this NMR sample was then obtained at 37 ^{o}C. The incubation at 37 ^{o}C causes a loss of helical content and the appearance of a strong band at ~217 nm (Figure 3B). After incubation at 37 ^{o}C, both the 2D ^{15}N-HSQC and CD spectra (Figure 3A,B) have a strong resemblance to the corresponding spectra of the urea induced pH 4 intermediate shown in Figures 1 and 2; although there is not a direct correspondence between amide resonances obtained at 30 ^{o}C in urea and those obtained at 37 ^{o}C in water. It was possible to obtain estimates of the amount of secondary structure from the CD spectra of the pH 4 intermediate at 37 ^{o}C using deconvolution algorithms. Anyalysis with the CDSSTR algorithms suggested 31% β-sheet present and only 3 % α-helix. However deconvolution analysis with the K2D secondary structure estimation program, 31 % β-sheet was indicated but as higher estimate of the α-helical content at 16%.

A 'head' count of the number of observable ^{15}N amides resonances in the pH 4 intermediate suggest a loss of some signals; from ~150 native full-length PrP (207 amino acids minus prolines and octarepeat degeneracy of signals) to half that in the pH 4 intermediate. Both the urea and temperature induced pH 4 intermediate shows a loss of half the amide cross-peaks but no loss of amide signal intensity. Using the 2D ^{15}N HSQC alone it was not clear if this loss of signals was due to signal overlap in the less dispersed spectra or the possibility that only a portion of the PrP was detected by the 2D ^{15}N HSQC in the pH 4 intermediate. The formation of a high molecular weight soluble polymeric species would become largely undetectable in the 2D ^{15}N-HSQC experiment due to their increase line-widths. Alternatively the formation of a molten-globule conformation could cause exchange-broadening of many signals. The retention of signals attributable to the Trp side-chain and Gly residues (for both the urea unfolded and the temperature induced pH intermediate) hints strongly at the possibility that only the N-terminal half of the protein is being detected. As the majority of Trp and Gly residues occur within the N-terminal half of the protein; residues 23-118 contain 27 out of 35 Glys and 7 out the 8 Trp residues of mouse PrP.

Truncated PrP, residues (113-231)- To test this hypothesis, PrP(113-231), a truncated version of full-length PrP was studied. This fragment lacks nearly all the unstructured N-terminal residues of native PrP^C. Similar truncated fragments have been shown to form a pH 4 intermediate [18, 19]. Figure 3 presents a comparison the the pH 4 intermediate for full-length PrP(23-231) to that of PrP(113-213). There is a dramatic change in the appearance of the 2D ^{15}N HSCQ spectrum for the truncated PrP(112-231) pH 4 intermediate, with only a few residues (~16 amide signals) being detected. This observation strongly suggests that the 2D ^{15}N HSQC of full-length PrP for the pH 4 intermediate only detects N-terminal residues (23–121). This is confirmed in the following section using 3D ^{15}N-HSQC-TOCSY and ^{15}N-HSQC-NOESY assignment methods.

Estimates of the secondary structure for the PrP(113-231) pH 4 intermediate from the CD spectra using CDSSTR fitting suggest that it is composed of ~46 % β-sheet, 27% turns and 23 % random and almost no α-helix (5%). However the K2D secondary structure estimates suggests that the pH 4 intermediate contains as much as 21 % α-helix and 31% β-sheet.

Main Chain NMR Assignments for the pH 4 intermediate- In order to understand the ^{15}N HSQC spectra further 3D ^{15}N-edited HSQC-TOCSY and NOESY experiments were obtained for the pH 4 intermediate for mPrP(23-231) in water at 37 ^{o}C. Almost all of the observed amide resonances from the ^{15}N HSQC have been assigned. All assigned resonances come from the N-terminus, between residues G30-G118 and are indicated on the ^{15}N HSQC, Figure 3a. Taken from

the 3D ^{15}N- HSQC-NOESY spectra, a section of a strip-plot, for residues T94-N107 is shown in Figure 4, sequential NOEs are indicated. There are a limited number of missing assignments, between G29-G118 attributed to glycine residues. The N-terminus contains a high percentage of GG sequences, which contributes to the overlap and makes a number of glycine amide peaks ambiguous to assign. Amide resonances within the four octa-repeats are degenerate and have four times the signal intensity of other amide signals. In addition, there are a further 4 amide peaks with observable TOCSY side-chain resonances, these amides lack appreciable NOE connectivities but can tentatively be attributed to Lys and Arg residues at the N-terminus, residues K23 to K27.

Chemical shift values have minimal deviations from 'random-coil'. For example, there are no Hα deviations that exceed 0.15 ppm and the overwhelming majority have deviation less than 0.1 ppm. Chemical shift indexing (CSI) criteria [43, 44] indicate that all the residues, 23-118, are indeed unstructured in the pH 4 intermediate (37 ^{o}C). Hα chemical shift assignments and deviations from random coil are available as supplementary material. We note that signals up to residue 115 are quite intense, comparable to intense signals from native PrP^{C}(23-231). Resonances for A117 and G118 have strongly attenuated signals while residues beyond 118 are not observed, due to the increased line-widths of these signals.

The ^{15}N HSQC spectrum for mPrP(113-231), pH 4, 37 ^{o}C (Figure 3C) shows a large reduction in the number of observed amide resonances only ~16 amide signals are observed. A number of these signals directly overlay with residues 114-118 from the pH 4 β-intermediate of mPrP(23-231).

Signal intensities of the β-intermediate in the 2D ^{15}N-HSQC spectra are very similar to that of the native 2D ^{15}N-HSQC, indicating that the majority of the protein is detected in the pH 4 2D ^{15}N-HSQC. A single set of resonances are observed for each spin-system, between residues 23 to 118. Based on peak intensity more than 90% of the protein is detected by the 2D ^{15}N-HSQC spectra of the pH 4 intermediate. This is true even when the more intense signals in the unstructured tail of native PrP^{C} are compared to resolved resonances of the β-intermediate.

Formation of the pH 4 intermediate is reversible and not subject to proteolytic cleavage-

There remained the possibility, albeit unlikely given the presence of a bacterial inhibitor reagent sodium-azide, that the detection of the N-terminal residues in the mPrP(23-231) pH 4 intermediate is the result of proteolytic cleavage of PrP under these conditions. However the SDS-PAGE of the native, pH 4 intermediate and the refolded native PrP(23-231) samples all showed intact PrP with

no appreciable cleavage products (see supplementary data). Further studies indicate that the formation of the pH 4, 37 ^{o}C, β-intermediate is reversible.

Furthermore, taking the pH 4 intermediate of mPrP(113-231) back to pH 5.5 causes the reappearance of an appreciable amounts of natively folded mPrP(113-231), as indicated by the 2D ^{15}N-HSQC spectra and UV-CD spectra shown in Figure 5.

^{15}N Transverse relaxation times of mPrP(23-231)- We then went on to characterize the molecular dynamics of the soluble PrP pH 4 intermediate using ^{15}N transverse (T_2) relaxation measurements. R_2 relaxation is sensitive to the overall rotational correlational time (τ_c) of a molecule. The presence of additional main-chain flexibility on a nano-to-pico second timescale can reduce R_2 values considerably.

R_2 relaxation values for amide resonances of the native mouse PrP(23-231) are comparable to values reported for full-length Syrian hamster PrP [7, 45] as would be expected. For example, typical ^{15}N R_2 relaxation values for amide resonances in helix A, B and C were 12-19 s^{-1} for full-length Syrian hamster PrP at 30 °C [7]. In this study, amides in the same region of mouse PrP(23-231) gave comparable R_2 values, e.g. 13.2, 16.7 and 18.7 s^{-1} for Y156, K203 and R207 respectively. In addition, amides from the unstructured tail (residues 29-120) gave R_2 values of ~4 s^{-1} [7]. Similar values are obtained here for mouse PrP(23-231), for example, A112 has an R_2 of 3.0 s^{-1}.

R_2 values for individual resonances for the pH 4 intermediate (3.5 M urea) were nearly all below 4 s^{-1}; typically 3.6 s^{-1}. These R_2 values are considerably smaller than those of a folded protein ~200 amino acids in size. It is clear R_2 values are dominated by local pico-second timescale motions indicating a high degree of flexibility of the N-terminal half of the protein, residues 23-114.

Translational diffusion measurements of mPrP(23-231)- Translational diffusion measurements can indicate the hydro-dynamic radius or molecular size of a protein. The techniques measures the bulk property of the protein rather than local internal motions. Using translational diffusion to indicate the molecular size of the β-intermediate has some advantages over previous methods such as size exclusion chromatography, as the studies are performed in solution under conditions similar to that used for the CD measurements. The intensities of the ^{15}N HSQC signals indicate for the N-terminal residues all the protein is being detected and not a small monomeric fraction. Figure 6 shows the ^{1}H spectra for native PrP acquired at different gradient strengths used to calculate the translational diffusion for PrP(23-231) in the 3 states; native, β-intermediate and

acid denatured. The translational diffusion coefficient (D_t) of native PrP(23-231) in 20 mM sodium acetate at pH 5.23 and 30 °C was 0.78±0.01× 10^{-6} cm^2 s^{-1}. This value is identical to the D_t value reported by workers for Syrian hamster PrP(29-231) and is typical for a monomeric protein of this size [7].

The D_t for mPrP(23-231) in 3.5 M Urea, 150 mM NaCl at pH 4.4 (the β-intermediate form) was 0.81±0.02 × 10^{-6} cm^2 s^{-1}. This is a value corrected for the increased viscosity due to the presence of 3.5 M Urea. The close similarity of the β-intermediate D_t value to that of native mPrP(23-231) indicated that the protein in its β-intermediate form is also predominantly monomeric. Uncorrected, the D_t (0.66±0.02 × 10^{-6} cm^2 s^{-1}) of the β-intermediate is comparable to that for dimeric PrP.

The D_t for mPrP(23-231) in 3.5 M Urea, 150 mM NaCl at pH 1.65 (the acid denatured form) was 0.50±0.01 × 10^{-6} cm^2 s^{-1}. The D_t for the acid denatured form, after correcting for the increased viscosity of the solution due to the presence of urea, was 0.61±0.01 × 10^{-6} cm^2 s^{-1}. The decreased D_t of the acid denatured mPrP(23-231) compared to the other 2 forms may indicate that it has aggregated into an oligomer. It is possible to calculate the increase in frictional coefficient, *f,* upon going from a monomer to an oligomer of *n* subunits [46]. The frictional coefficient of a molecule is related to the reciprocal of its translational diffusion by the Stokes Einstein equation; $D_t = k_BT/f$, in which k_B is the Boltzmann constant and T is the absolute temperature [37, 46]. The increase in *f* upon going from a monomer to an oligomer of *n* subunits for different values of *n* have been calculated using the equation: $F_n = n^{1/3}(f_m/f_n)$, F_n is a geometric factor, *n* is the number of subunits in the oligomer while f_m and f_n are the frictional coefficients of the monomer and oligomer respectively [46]. The experimental D_t ratio of the acid denatured form of mPrP(23-231) to that of native mPrP(23-231) in this study is 0.78. This ratio is very similar to a D_t ratio of 0.75 expected for a theoretical monomer dimer model, note the analyses assumes a globular (spherical) oligomer [46]. It is also similar to an experimental D_t ratio of 0.72 for the monomer/dimer system of ubiquitin and of the dimeric cytokine MCP-1 proteins [37]. Thus the translational diffusion data indicates that the native and β-intermediate forms of mPrP(23-231) are predominantly monomeric while the D_t of the acid denatured form implies a dimer.

The translational diffusion coefficient for the PrP sample obtained for the pH 4 intermediate at 37 ^oC but without urea present, exhibits a D_t of 0.62±0.02 × 10^{-6} cm^2s^{-1}. This value did not need to be corrected for the viscosity of urea as the denaturant was not present. The pH 4 intermediate, produced under these conditions, gives a translation diffusion coefficient close to that expected for a

dimer of PrP. However correction for the increased temperature (37 ^{o}C) gave a value of 0.54 x 10^{-6} cm^2 s^{-1}. This value might suggest a larger molecule close to a trimer in size. These diffusion coefficients represent an average value for the PrP oligomer in equilibrium between monomer and higher mol weight species. Small amounts of monomer would have the effect of increasing the average rate of translational diffusion while large oligomers would have the opposite effect.

Discussion

For the first time the nature of the prion protein pH 4 β-intermediate, has been characterized on a per-residue basis. The NMR chemical shifts and assignments of the β-intermediate indicate that the majority of prion protein molecules within a pH 4 oligomer possess a long flexible tail incorporating residues 23-118. The exact nature of the C-terminal half of PrP remains elusive as large line-widths have rendered these residues undetectable by NMR. However deconvolution of the CD spectra indicate a high proportion of β-sheet for this region 31-46% β-sheet for PrP(113-231). The variability in the secondary structure estimates by CD is perhaps due to the nature of the oligomer, which may contain extended conformations in a molten globule state. Standard secondary structure elements used by the algorithms will therefore fit poorly to the observed spectra. Protein oligomers have a tendency to form extended conformations that produce CD spectra with a negative CD band at ~217 nm similar to that observed for β-sheet proteins. It is therefore not clear if either an extended β-like polypeptide chain, or a more ordered hydrogen bonded net-work, found in cross β-sheets of amyloids, is present in the beta intermediate. It is clear that the formation of the soluble pH 4 oligomer is reversible, returning the pH to 5.5 results in the refolding of the monomeric native species.

The studies described here have been carried out with the native disulphide bond intact. It is generally believed the PrP^{Sc} exists with the native disulphide bond present [47]. A model of amyloids of PrP^{Sc} based predominantly on EM data suggests that much of helix B and C remains intact in the fibrils while residues 89-174 forms a cross-β structure in a β-helix conformation [48]. FTIR spectroscopy suggests that some of the α-helical structure is retained in the pH 4 oligomeric species [24]. Estimates of α-helix content from the CD spectra, (although variable) between 3 and 21 %) suggest there is little α-helix content for the pH 4 intermediate. It remains to be established if helices remain in the pH 7 amyloid species.

The translational diffusion measurements suggest that the β-intermediate is a trimer in size. This is a surprise as a number of studies using guanidine hydrochloride, urea or elevated temperature as partial denaturants have indicated that the pH 4 β-intermediate is oligomeric. Investigations using size exclusion chromatography and dynamic light scattering measurements suggest that this β-intermediate is ~octameric [20, 21, 23]. Multi-angle laser light scattering experiments suggest that this oligomeric species contains 8-15 monomers [24] small angle X-ray scattering has also indicated a large oligomer [25]. Our own 2D ^{15}N-HSQC spectra indicate a complete loss of signal from the C-terminus of PrP suggesting a molecule of high molecular weight which renders the signal too broad for detection. However we do note that a loss of signal might also be due to exchange broadening due to slow milli-micro second motions of the main-chain of the C-terminal domain in a molten globule state. The translational diffusion value represents a weighted average of various oligomeric species, however the presence of for example, 10 % monomer would not reduce the D_t value by a significant amount.

Residues 90-121 have been shown to be essential for prion propagation suggesting that a conformational change in this region is key to prion propagation [49, 50]. Furthermore a number of mutations associated with familial prion diseases are also found in this region. However in native PrP these residues are unstructured despite structure prediction studies of native PrP that suggest that residues 109-122 might form an α-helix. Models of PrP^{Sc} suggest that residues 89-174 might form a β-helical structure [48]. However interestingly as with native PrP these residues (23-118) remain unstructured with a high degree of flexibility in the soluble pH 4 β-intermediate.

Characterizing folding intermediates of the prion protein is an important goal towards understanding the mechanism of prion replication. For example it has been shown that the rate of formation of the pH 4 β-intermediate is influenced by polymorphism at residue 129. Met129 has a higher propensity to form the pH 4 β-intermediate than Val129 [28]. Interestingly, to date only individuals homozygous for methionine (Met/Met) have contracted variant CJD.

Acknowledgements- This work was funded by BBSRC Project Grants. C.E.J. is the recipient of a C.J. Martin Postdoctoral Fellowship from the National Health and Medical Research Council, Australia. Thanks to Macus Fries for assistance with the SDS-PAGE.

Figure legends

Figure 1. 2D ^{15}N-HSQC spectra of mouse PrP(23-231) (A) pH 5.21, 20 mM sodium acetate (B) pH 4.11, 3.5 M Urea, 150 mM NaCl, 20 mM sodium acetate (C) pH 1.65, 3.5 M Urea, 150 mM NaCl, 20 mM sodium acetate. Concentration of His tagged PrP(23-231) ~5 mg/ml, spectra were recorded at 30 ^{o}C.

Figure 2. UV-CD spectra of mPrP(23-231): (A) pH 5.1, 20 mM sodium acetate (B) pH 3.9, 3.5 M Urea, 150 mM NaCl, 20 mM sodium acetate (C) pH 1.65, 3.5 M Urea, 150 mM NaCl, 20 mM sodium acetate (dashed line). Concentration of His tagged PrP(23-231) samples are 0.4 mg/ml, spectra were recorded at 25 ^{o}C with a 0.02 cm path length.

Figure 3. **2D ^{15}N-HSQC and UV-CD spectra of two mPrP constructs at pH ~4.** (A) ^{15}N HSQC recorded after 2 hours incubation at 37 ºC of his-tag-free mPrP(23-231) at pH 3.6, 20 mM sodium acetate. [PrP(23-231) ~5 mg/ml]. Peaks are assigned based on 3D ^{15}N-edited HSQC-TOCSY and –NOESY data. Unlabelled peaks had no NOE connectivities. The dashed box surrounds Q/N side-chain amine resonances. (B) CD spectra of mPrP(23-231), pH 3.6 at 37 ºC and pH 5.1 at 25 ºC . (C) ^{15}N HSQC, recorded after 18 hours incubation at 37 ºC of PrP(113-231) ~3 mg/ml pH 3.9. Resonances that directly overlap peaks in (A) are highlighted and (D) CD spectra of mPrP(113-231) at, pH 3.9 and pH 5.2 at 37 ºC.

Figure 4: 3D ^{15}N-HSQC-NOESY strip-plot of mPrP(23-231) at pH 4.0 at 37 ^{o}C. Residues T94 to N107 are shown, side-chain assignments also observed in 3D TOCSY are indicated, as are sequential NOE's.

Figure 5: **2D ^{15}N-HSQC and associated CD spectra for refolded mPrP(113-231)**. (A) Native pH 5.2 , 37 ^{o}C (B) β-intermediate pH 3.9, 37 ^{o}C (C) refolded native from pH 5.3 (taken from the pH 3.9, 37 ^{o}C β-intermediate).

Figure 6. Translational diffusion measurements of mPrP(23-231) in its native, β-intermediate and acid denatured forms. (A) 1D ^{1}H NMR spectra of native mPrP(23-231) (6 mg/ml) using stimulated echo with increasing field gradient strength between 28.3 and 12.2 G/cm. (B) The natural log of the peak intensity for the aromatic region of the spectra was plotted against the corresponding square of the gradient strengths. Least square straight line fit to: (i) native state pH

5.2 (circle), (ii) pH 4.40, 3.5 M Urea, 150 mM NaCl (square) (iii) pH 1.64, 3.5 M Urea, 150 mM NaCl (diamond), (iv) pH 3.67 after incubation at 37 ^{o}C (triangle).

References

1 Prusiner, S. B. (1998) Prions. Proc Natl Acad Sci U S A **95**, 13363-83

2 Legname, G., Baskakov, I. V., Nguyen, H. O., Riesner, D., Cohen, F. E., DeArmond, S. J. and Prusiner, S. B. (2004) Synthetic mammalian prions. Science **305**, 673-6

3 Riek, R., Hornemann, S., Wider, G., Billeter, M., Glockshuber, R. and Wuthrich, K. (1996) NMR structure of the mouse prion protein domain PrP(121-321). Nature **382**, 180-2

4 James, T. L., Liu, H., Ulyanov, N. B., Farr-Jones, S., Zhang, H., Donne, D. G., Kaneko, K., Groth, D., Mehlhorn, I., Prusiner, S. B. and Cohen, F. E. (1997) Solution structure of a 142-residue recombinant prion protein corresponding to the infectious fragment of the scrapie isoform. Proc. Natl. Acad. Sci. USA **94**, 10086-91

5 Donne, D. G., Viles, J. H., Groth, D., Mehlhorn, I., James, T. L., Cohen, F. E., Prusiner, S. B., Wright, P. E. and Dyson, H. J. (1997) Structure of the recombinant full-length hamster prion protein PrP(29-231): the N terminus is highly flexible. Proc. Natl. Acad. Sci. USA **94**, 13452-7

6 Riek, R., Wider, G., Billeter, M., Hornemann, S., Glockshuber, R. and Wuthrich, K. (1998) Prion protein NMR structure and familial human spongiform encephalopathies. Proc Natl Acad Sci U S A **95**, 11667-72

7 Viles, J. H., Donne, D., Kroon, G., Prusiner, S. B., Cohen, F. E., Dyson, H. J. and Wright, P. E. (2001) Local structural plasticity of the prion protein. Analysis of NMR relaxation dynamics. Biochemistry **40**, 2743-53

8 Brown, D. R., Qin, K., Herms, J. W., Madlung, A., Manson, J., Strome, R., Fraser, P. E., Kruck, T., von Bohlen, A., Schulz-Schaeffer, W., Giese, A., Westaway, D. and Kretzschmar, H. (1997) The cellular prion protein binds copper in vivo. Nature **390**, 684-7

9 Viles, J. H., Cohen, F. E., Prusiner, S. B., Goodin, D. B., Wright, P. E. and Dyson, H. J. (1999) Copper binding to the prion protein: structural implications of four identical cooperative binding sites. Proc Natl Acad Sci U S A **96**, 2042-7

10 Jones, C. E., Klewpatinond, M., Abdelraheim, S. R., Brown, D. R. and Viles, J. H. (2005) Probing copper2+ binding to the prion protein using diamagnetic nickel2+ and 1H NMR: the unstructured N terminus facilitates the coordination of six copper2+ ions at physiological concentrations. J Mol Biol **346**, 1393-407

11 Garnett, A. P. and Viles, J. H. (2003) Copper binding to the octarepeats of the prion protein. Affinity, specificity, folding, and cooperativity: insights from circular dichroism. J Biol Chem **278**, 6795-802

12 Jones, C. E., Abdelraheim, S. R., Brown, D. R. and Viles, J. H. (2004) Preferential Cu2+ Coordination by His96 and His111 Induces {beta}-Sheet Formation in the Unstructured Amyloidogenic Region of the Prion Protein. J Biol Chem **279**, 32018-32027

13 Meyer, R. K., McKinley, M. P., Bowman, K. A., Braunfeld, M. B., Barry, R. A. and Prusiner, S. B. (1986) Separation and properties of cellular and scrapie prion proteins. Proc Natl Acad Sci U S A **83**, 2310-4

14 Stahl, N. and Prusiner, S. B. (1991) Prions and prion proteins. Faseb J **5**, 2799-807

15 Cohen, F. E. and Prusiner, S. B. (1998) Pathologic conformations of prion proteins. Annu Rev Biochem **67**, 793-819

16 Caughey, B. W., Dong, A., Bhat, K. S., Ernst, D., Hayes, S. F. and Caughey, W. S. (1991) Secondary structure analysis of the scrapie-associated protein PrP 27-30 in water by infrared spectroscopy. Biochemistry **30**, 7672-80

17 Pan, K. M., Baldwin, M., Nguyen, J., Gasset, M., Serban, A., Groth, D., Mehlhorn, I., Huang, Z., Fletterick, R. J., Cohen, F. E. and et al. (1993) Conversion of alpha-helices into beta-sheets features in the formation of the scrapie prion proteins. Proc Natl Acad Sci U S A **90**, 10962-6

18 Hornemann, S. and Glockshuber, R. (1998) A scrapie-like unfolding intermediate of the prion protein domain PrP(121-231) induced by acidic pH. Proc Natl Acad Sci U S A **95**, 6010-4

19 Swietnicki, W., Petersen, R., Gambetti, P. and Surewicz, W. K. (1997) pH-dependent stability and conformation of the recombinant human prion protein PrP(90-231). J Biol Chem **272**, 27517-20

20 Swietnicki, W., Morillas, M., Chen, S. G., Gambetti, P. and Surewicz, W. K. (2000) Aggregation and fibrillization of the recombinant human prion protein huPrP90-231. Biochemistry **39**, 424-31

21 Morillas, M., Vanik, D. L. and Surewicz, W. K. (2001) On the mechanism of alpha-helix to beta-sheet transition in the recombinant prion protein. Biochemistry **40**, 6982-7

22 Baskakov, I. V., Legname, G., Baldwin, M. A., Prusiner, S. B. and Cohen, F. E. (2002) Pathway complexity of prion protein assembly into amyloid. J Biol Chem **277**, 21140-8

23 Baskakov, I. V., Legname, G., Prusiner, S. B. and Cohen, F. E. (2001) Folding of prion protein to its native alpha-helical conformation is under kinetic control. J Biol Chem **276**, 19687-90

24 Vendrely, C., Valadie, H., Bednarova, L., Cardin, L., Pasdeloup, M., Cappadoro, J., Bednar, J., Rinaudo, M. and Jamin, M. (2005) Assembly of the full-length recombinant mouse prion protein I. Formation of soluble oligomers. Biochim Biophys Acta **1724**, 355-66

25 Rezaei, H., Eghiaian, F., Perez, J., Doublet, B., Choiset, Y., Haertle, T. and Grosclaude, J. (2005) Sequential generation of two structurally distinct ovine prion protein soluble oligomers displaying different biochemical reactivities. J Mol Biol **347**, 665-79

26 Hosszu, L. L., Jackson, G. S., Trevitt, C. R., Jones, S., Batchelor, M., Bhelt, D., Prodromidou, K., Clarke, A. R., Waltho, J. P. and Collinge, J. (2004) The residue 129 polymorphism in human prion protein does not confer susceptibility to Creutzfeldt-Jakob disease by altering the structure or global stability of PrPC. J Biol Chem **279**, 28515-21

27 Baskakov, I., Disterer, P., Breydo, L., Shaw, M., Gill, A., James, W. and Tahiri-Alaoui, A. (2005) The presence of valine at residue 129 in human prion protein accelerates amyloid formation. FEBS Lett **579**, 2589-96

28 Tahiri-Alaoui, A., Gill, A. C., Disterer, P. and James, W. (2004) Methionine 129 variant of human prion protein oligomerizes more rapidly than the valine 129 variant: implications for disease susceptibility to Creutzfeldt-Jakob disease. J Biol Chem **279**, 31390-7

29 Collinge, J., Sidle, K. C., Meads, J., Ironside, J. and Hill, A. F. (1996) Molecular analysis of prion strain variation and the aetiology of 'new variant' CJD. Nature **383**, 685-90

30 Silveira, J. R., Raymond, G. J., Hughson, A. G., Race, R. E., Sim, V. L., Hayes, S. F. and Caughey, B. (2005) The most infectious prion protein particles. Nature **437**, 257-61

31 Wong, B. S., Wang, H., Brown, D. R. and Jones, I. M. (1999) Selective oxidation of methionine residues in prion proteins. Biochem Biophys Res Commun **259**, 352-5

32 Gill, S. C. and von Hippel, P. H. (1989) Calculation of protein extinction coefficients from amino acid sequence data. Anal Biochem **182**, 319-26

33 Kay, L., Keifer, P. and Saarinen, T. (1992) Pure absorption gradient enhanced heteronuclear single quantum correlation spectroscopy with improved sensitivity. J. Am. Chem. Soc. **114**, 10663 - 10665

34 Zhang, O., Kay, L. E., Olivier, J. P. and Forman-Kay, J. D. (1994) Backbone 1H and 15N resonance assignments of the N-terminal SH3 domain of drk in folded and unfolded states using enhanced-sensitivity pulsed field gradient NMR techniques. J Biomol NMR **4**, 845-58

35 Farrow, N. A., Muhandiram, R., Singer, A. U., Pascal, S. M., Kay, C. M., Gish, G., Shoelson, S. E., Pawson, T., Forman-Kay, J. D. and Kay, L. E. (1994) Backbone dynamics of a free and phosphopeptide-complexed Src homology 2 domain studied by 15N NMR relaxation. Biochemistry **33**, 5984-6003

36 Viles, J. H., Duggan, B. M., Zaborowski, E., Schwarzinger, S., Huntley, J. J., Kroon, G. J., Dyson, H. J. and Wright, P. E. (2001) Potential bias in NMR relaxation data introduced by peak intensity analysis and curve fitting methods. J Biomol NMR **21**, 1-9

37 Altieri, A. S., Hinton, D. P. and Byrd, R. A. (1995) Association of Biomolecular Systems via Pulsed Field Gradient NMR Self-Diffusion Measurements. J. Am. Chem. Soc. **117**, 7566-7567

38 Stejskal, E. O. and Tanner, J. E. (1965) Spin Diffusion Measurements: Spin Echoes in the Presence of a Time-Dependent Field Gradient. J. Chem. Phys. **42**, 288-292

39 Lobley, A., Whitmore, L. and Wallace, B. A. (2002) DICHROWEB: an interactive website for the analysis of protein secondary structure from circular dichroism spectra. Bioinformatics **18**, 211-2

40 Yao, J., Dyson, H. J. and Wright, P. E. (1997) Chemical shift dispersion and secondary structure prediction in unfolded and partly folded proteins. FEBS Lett **419**, 285-9

41 Eliezer, D., Yao, J., Dyson, H. J. and Wright, P. E. (1998) Structural and dynamic characterization of partially folded states of apomyoglobin and implications for protein folding. Nat. Struct. Biol. **5**, 148-55

42 Zhang, O. and Forman-Kay, J. D. (1995) Structural characterization of folded and unfolded states of an SH3 domain in equilibrium in aqueous buffer. Biochemistry **34**, 6784-94

43 Wishart, D. S., Sykes, B. D. and Richards, F. M. (1992) The chemical shift index: a fast and simple method for the assignment of protein secondary structure through NMR spectroscopy. Biochemistry **31**, 1647-51

44 Wishart, D. S. and Sykes, B. D. (1994) The 13C chemical-shift index: a simple method for the identification of protein secondary structure using 13C chemical-shift data. J Biomol NMR **4**, 171-80

45 Liu, H., Farr-Jones, S., Ulyanov, N. B., Llinas, M., Marqusee, S., Groth, D., Cohen, F. E., Prusiner, S. B. and James, T. L. (1999) Solution structure of Syrian hamster prion protein rPrP(90-231). Biochemistry **38**, 5362-77

46 Teller, D. C., Swanson, E. and de Haen, C. (1979) The translational friction coefficient of proteins. Methods Enzymol **61**, 103-24

47 Turk, E., Teplow, D. B., Hood, L. E. and Prusiner, S. B. (1988) Purification and properties of the cellular and scrapie hamster prion proteins. Eur J Biochem **176**, 21-30

48 Govaerts, C., Wille, H., Prusiner, S. B. and Cohen, F. E. (2004) Evidence for assembly of prions with left-handed beta-helices into trimers. Proc Natl Acad Sci U S A **101**, 8342-7

49 Muramoto, T., Scott, M., Cohen, F. E. and Prusiner, S. B. (1996) Recombinant scrapie-like prion protein of 106 amino acids is soluble. Proc Natl Acad Sci U S A **93**, 15457-62

50 Brown, D. R., Schmidt, B. and Kretzschmar, H. A. (1996) Role of microglia and host prion protein in neurotoxicity of a prion protein fragment. Nature **380**, 345-347

Biochemical Journal Immediate Publication. Published on 8 Sep 2006 as manuscript BJ20060668

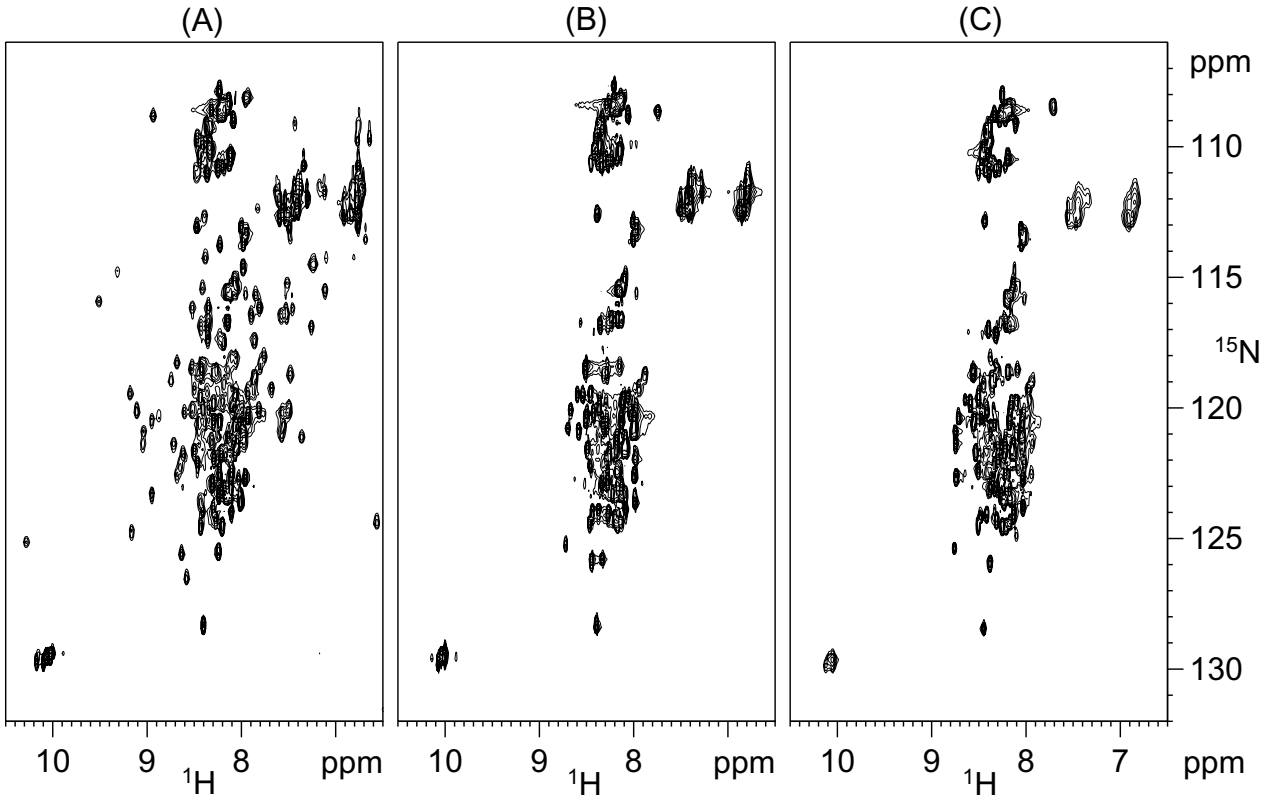

Figure 1: O' Sullivan/Jones/Viles

Biochemical Journal Immediate Publication. Published on 8 Sep 2006 as manuscript BJ20060668

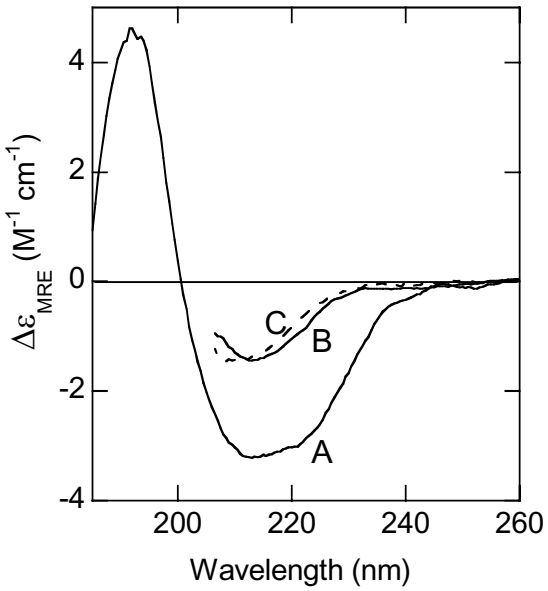

Figure 2: O' Sullivan/Jones/Viles

Biochemical Journal Immediate Publication. Published on 8 Sep 2006 as manuscript BJ20060668

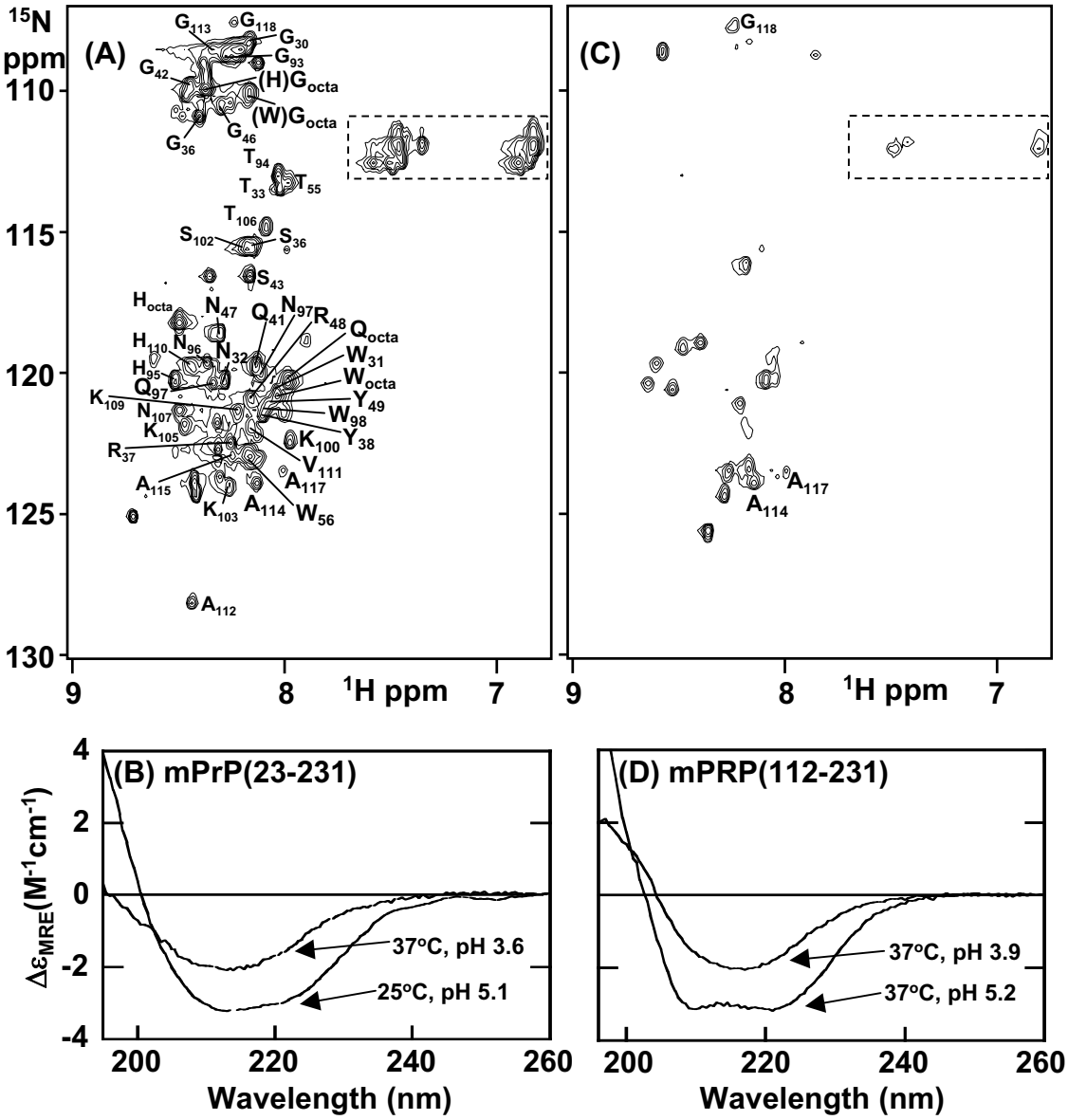

Figure 3: O' Sullivan/Jones/Viles

Biochemical Journal Immediate Publication. Published on 8 Sep 2006 as manuscript BJ20060668

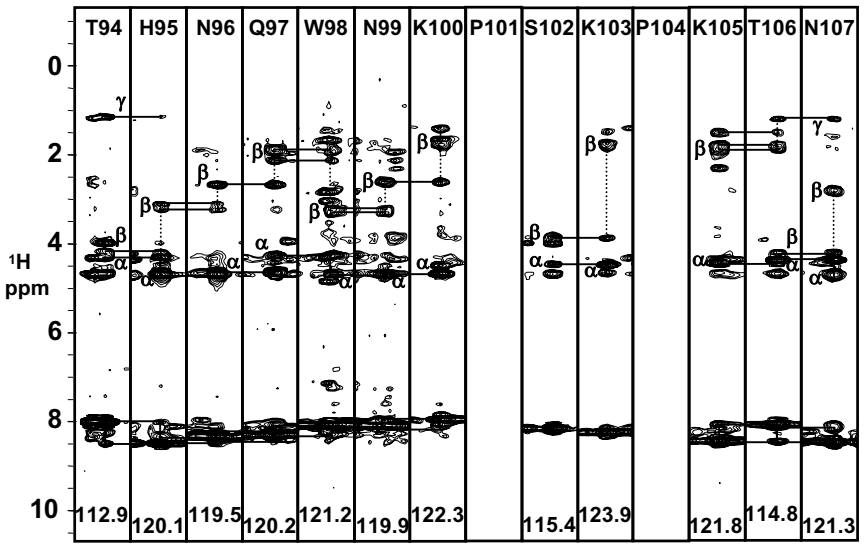

Figure 4 O' Sullivan/Jones/Viles

Biochemical Journal Immediate Publication. Published on 8 Sep 2006 as manuscript BJ20060668

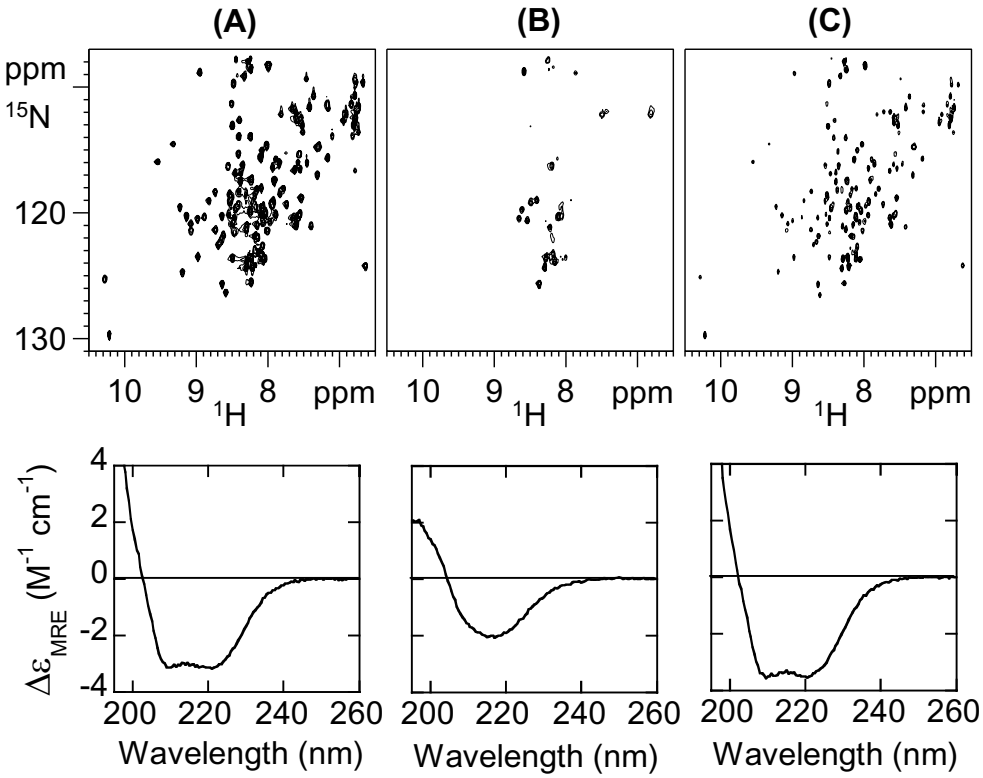

Figure 5 O' Sullivan/Jones/Viles

Biochemical Journal Immediate Publication. Published on 8 Sep 2006 as manuscript BJ20060668

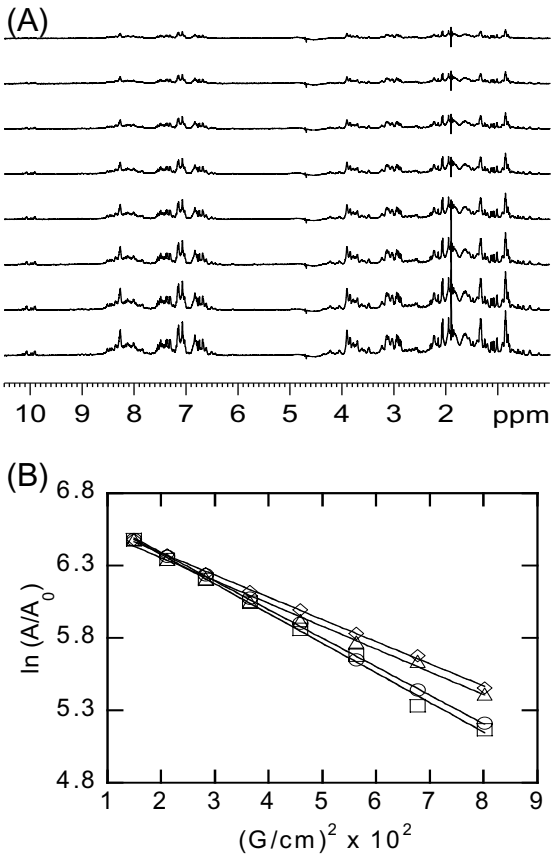

Figure 6: O' Sullivan/Jones/Viles